A R C H I V E S O F M E T A L L U R G Y A N D M A T E R I A L S
Volume 50 2005 Issue 2

M. WITKOWSKA*, J. RYŚ*, W. RATUSZEK*, A. ZIELIŃSKA-LIPIEC*

ANNEALING TEXTURES AND PRECIPITATION BEHAVIOUR IN FERRITIC-AUSTENITIC DUPLEX TYPE STEELS

TEKSTURY WYŻARZANIA I PROCESY WYDZIELANIA W STALACH FERRYTYCZNO-AUSTENITYCZNYCH TYPU DUPLEX

Development of annealing textures and precipitation behaviour in the course of recrystallization annealing were examined in two ferritic-austenitic stainless steels of duplex type; 00H18N6Mo3 and 00H24N6. Following thermo- mechanical pre-treatment both steels were cold-rolled up to high reductions and subsequently annealed within the temperature range 700÷950°C. Texture changes in the course of annealing resulted from recovery and / or recrystallization processes within the bands of both phases, precipitation of sigma phase and secondary austenite due to the decomposition of ferrite. Differences in ferrite and austenite texture development between both duplex steels are attributed to different contribution of these processes depending on temperature and time of annealing. Contribution of the inverse ($\alpha \rightarrow \gamma$) transformation into texture formation results from the amount of strain induced α-phase, which depends on chemical composition and phase stability.

Badania dotyczyły rozwoju tekstur wyżarzania i procesów wydzielania podczas wyżarzania rekrystalizującego dwóch nierdzewnych stali ferrytyczno-austenitycznych typu duplex, 00H18N6Mo3 oraz 00H24N6. Po wstępnej obróbce cieplno-mechanicznej obie stale walcowano na zimno do wysokich odkształceń a następnie wyżarzano w zakresie temperatur 700÷950°C. Zmiany tekstury w trakcie wyżarzania wynikały z procesów zdrowienia i / lub rekrystalizacji w obszarach pasm obu faz, wydzielania fazy sigma i austenitu wtórnego na skutek rozpadu ferrytu. Różnice pomiędzy obiema stalami w rozwoju tekstur ferrytu i austenitu przypisywane są różnemu udziałowi tych procesów zależnie od temperatury i czasu wyżarzania. Udział przemiany odwrotnej ($\alpha \rightarrow \gamma$) w tworzeniu tekstury wynika z ilości fazy-α indukowanej odkształceniem i uzależniony jest od składu chemicznego i stabilności fazowej.

* WYDZIAŁ METALURGII I INŻYNIERII MATERIAŁOWEJ, AKADEMIA GÓRNICZO-HUTNICZA, 30-059 KRAKÓW, AL. MICKIEWICZA 30

1. Introduction

A number of processes contribute to the structure and texture formation in ferritic-austenitic stainless steel sheets upon rolling and annealing treatment. Apart from the mechanisms of slip and / or twinning within the γ-phase and the multiple slip within the α-phase, plastic deformation may proceed by strain induced ($\gamma \rightarrow \alpha$) transformation [1, 2]. In the course of annealing, recovery and / or recrystallization processes of both phases may be accompanied by the inverse ($\alpha \rightarrow \gamma$) transformation and various precipitation processes, including the precipitation of sigma phase and secondary austenite due to the decomposition of ferrite ($\alpha \rightarrow \sigma + \gamma$) [3÷5]. Contribution of these processes into the texture development is affected by the band-like morphology of two-phase structure and depends on chemical and phase composition, initial crystallographic orientations, conditions of plastic working and annealing treatment.

2. Material and experimental procedure

The exact chemical compositions of two ferritic-austenitic stainless steels under examination, i.e. 00H18N6Mo3 and 00H24N6, are given in Table. Based on the metallographic analysis the ferrite volume fraction in both steels was estimated at about 60÷65%.

TABLE

Chemical composition of two-phase steels (in wt. %)

	Steel	C	Cr	Ni	Mo	Mn	Si	Al	S	P	N
A	00H18N6Mo3	0.008	18.43	6.33	2.95	1.47	1.63	—	0.020	0.010	0.018
B	00H24N6	0.009	23.7	6.0	—	1.23	0.34	0.02	0.010	0.008	0.012

The steel ingots were industrially homogenized and hot worked at the temperatures 900÷1000°C. Further processing included solution treatment at 1050°C, cold-rolling up to 85% and 90% of strain by applying high reductions per pass, and annealing over the range of temperatures 700÷950°C.

X-ray investigations included the phase analysis and texture measurements, from the centre layers of the sheets, conducted by means of Bruker diffractometer D8 Advance using Co Kα radiation. Texture examination was performed on the basis of the orientation distribution functions (ODFs) calculated from incomplete pole figures and the analysis of orientation fibres in both phases. Microstructure observations were carried out by means of Zeiss optical microscope Neophot-2, Cambridge scanning microscope Stereo-scan and Jeol electron microscope JEM 200 CX.

3. Results and discussion

Duplex type steels under examination showed different intensities of the initial textures after thermo-mechanical pre-treatment. **Steel A** (00H18N6Mo3) showed relatively strong cubic texture {100}<001> of ferrite and weak austenite texture with {110}<001> Goss component on a background of random orientation. **Steel B** (00H24N6) exhibited strong initial textures of ferrite and austenite with the dominant components {100}<001> and {110}<001> respectively and Bain relationship describing orientation relation between both phases [6, 7].

Significant differences in the intensity between the ferrite and austenite rolling textures occurred in **steel A** (Fig. 1), due to the strain induced ($\gamma \rightarrow \alpha$) transformation

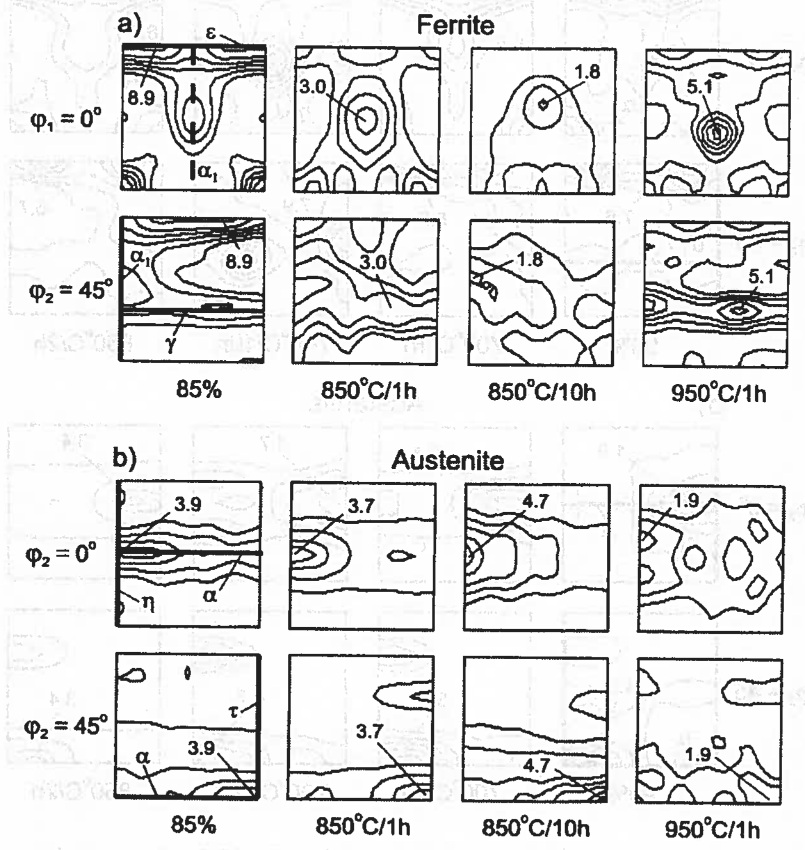

Fig. 1. Orientation distribution functions (ODFs) for steel A after 85% reduction and annealing at 850°C/1h, 850°C/10h and 950°C/1h in sections: φ_1 = 0°, φ_2 = 45° for ferrite **(a)** and φ_2 = 0° and ϕ_2 = 45° for austenite **(b)**

(temperature M_{d30} above 35°C). Some components of the strong ferrite rolling texture were generated through the Kurdjumov-Sachs (K-S) relation from the austenite texture [6]. The final rolling texture of ferrite after 85% reduction may be described by the non-homogeneous ε-fibre <001>|| ND, the limited α_1-fibre <110>|| RD and the relatively weak γ-fibre <111>|| ND. The strongest texture components are close to the {001}<310>÷<210> orientations from the ε-fibre (Fig.1a). In deformed austenite, only the non-homogeneous α-fibre <110>|| ND appeared in the final rolling texture, with the most pronounced texture components from the range {110}<001>÷<112>, i.e. between Goss and alloy-type orientations (Fig.1b) [6].

After cold-rolling of **steel B** differences in the intensity between the main texture components of both phases are smaller (Fig. 2). Texture measurements give no indica-

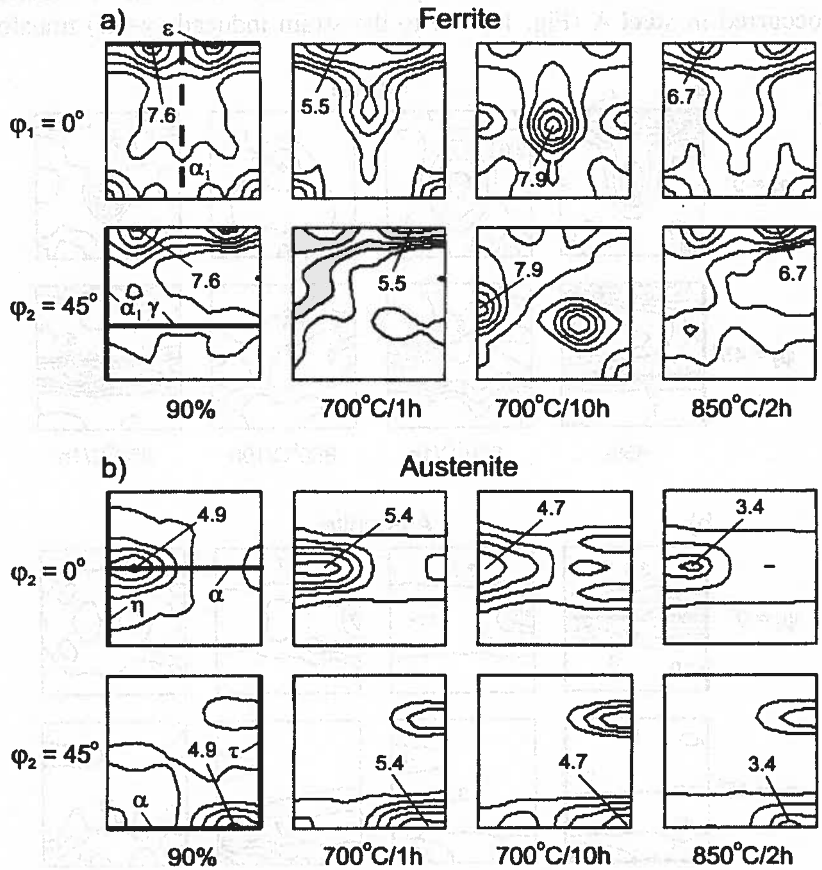

Fig. 2. Orientation distribution functions (ODFs) for steel B after 90% reduction and annealing at 700°C/1h, 700°C/10h and 850°C/2h in sections: $\varphi_1 = 0°$, $\varphi_2 = 45°$ for ferrite **(a)** and $\varphi_2 = 0°$ and $\varphi_2 = 45°$ for austenite **(b)**

tion of a significant role of strain induced phase transformation. Calculations based on the chemical composition of austenite indicate at M_{d30} temperature about 5°C. Higher intensity of the ferrite rolling texture in comparison to the austenite texture results mainly from the higher volume fraction of ferrite. Deformation of ferrite-austenite banded structure in **steel B** may be interpreted as plastically compatible and the {100}<001> cubic component and the {110}<001> Goss component remained within the rolling textures of the α- and γ- phases respectively up to high reductions [7]. At the absence of the γ- and α_1-fibres the ferrite rolling texture after 90% reduction describes the non-homogeneous ε-fibre. The strongest texture components are close to the {100}<012> orientations. The final rolling texture of austenite may be essentially described by the limited and spread α-fibre with the maximum intensity close to the {110}<115> orientation.

Upon annealing of **steel A** at the temperature 850°C/1h the intensity of the ferrite texture considerably decreases (Fig. 1a). After longer annealing time a decay of the α_1-, ε- and γ-fibres is observed. Strong weakening of certain components of the ferrite texture results from two processes, namely; the inverse ($\alpha \rightarrow \gamma$) transformation and the precipitation of σ-phase due to the decomposition of ferrite (Figs. 3a, 4). The

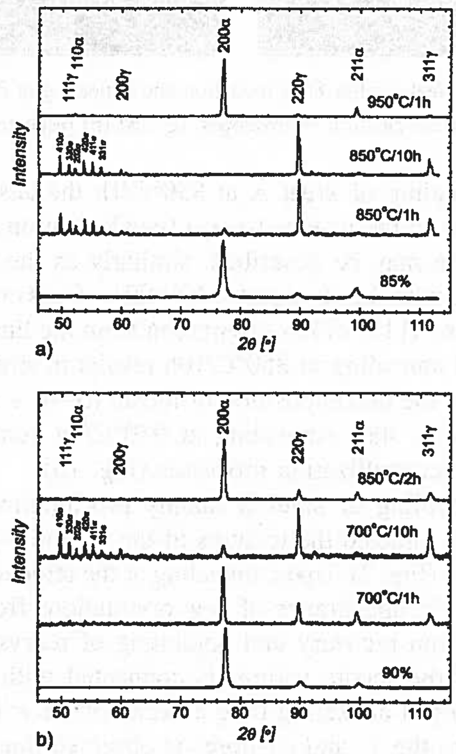

Fig. 3. X-ray diffraction patterns for duplex type steels A and B after 85% and 90% reduction and annealing as shown in (a) and (b) respectively

temperature range for σ-phase precipitation is shifted to higher temperatures due to presence of 3%Mo within the composition of steel A. The ferrite texture after annealing at 850°C/10h is nearly random with some weak and spread components laying close to the (112÷113)<110> orientations. Annealing treatment at 950°C/1h, i.e. above the temperature range for σ-phase precipitation, essentially increases the intensity of the ferrite texture. After recrystallization the texture of ferrite may be described by the non-homogeneous γ-fibre with the strongest component close to {111}<110> as well as the weak ε- fibre.

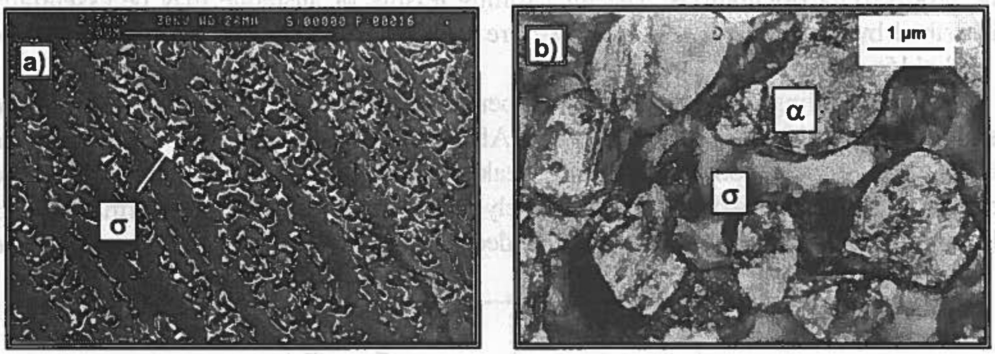

Fig. 4. Microstructures of steel A after 85% reduction and annealing at 850°C/1h; scanning and transmission electron microscopes, (a) and (b) respectively

As the result of annealing of **steel A** at 850°C/1h the austenite initially inherits its own rolling texture due to the inverse ($\alpha \rightarrow \gamma$) transformation (Fig. 1b) [8]. Thus the austenite annealing texture may be described, similarly as the rolling texture, by the non-homogeneous α-fibre with the strongest {110}<001> Goss component. Additionally the components close to the {113}<332> orientation from the limited {113}<uvw>-fibre were detected. Prolonged annealing at 850°C/10h results in strengthening of austenite texture, most likely due to the decomposition of ferrite ($\alpha \rightarrow \sigma + \gamma_2$) and the appearance of secondary austenite (Fig. 4a). Annealing at 950°C/1h considerably weakens the austenite texture due to recrystallization processes (Fig. 1b).

In the course of annealing of **steel B** mainly precipitation of sigma phase and recrystallization processes affected the textures of the α- and γ-phases with a stronger effect on the ferrite texture (Fig. 2). Upon annealing at the temperature 700°C/1h preservation of the ε-fibre and the appearance of new orientations from the limited α_1-fibre in ferrite texture result from recovery and beginning of recrystallization respectively (Fig. 2a). Weakening of the ferrite texture is connected with the onset of σ-phase precipitation. With prolonged annealing time a decay of the ε-fibre and strengthening of some components from the γ- and α_1-fibres is observed due to the precipitation of σ-phase and recrystallization of ferrite (Figs. 3b and 5). After annealing at 700°C/10h the strongest component in the ferrite texture is close to the {556}<110> orientation from the α_1-fibre. Another strongly pronounced texture component is close to the {111}<110> orientation from the γ-fibre. In the case of steel B (without molybdenum) the temperature 850°C lays above the temperature range for sigma phase precipitation (Fig. 3b). The texture of ferrite after annealing at 850°C/2h results from recovery and the onset of recrystallization and does not exhibit considerable changes in comparison to the rolling texture (Fig. 2a).

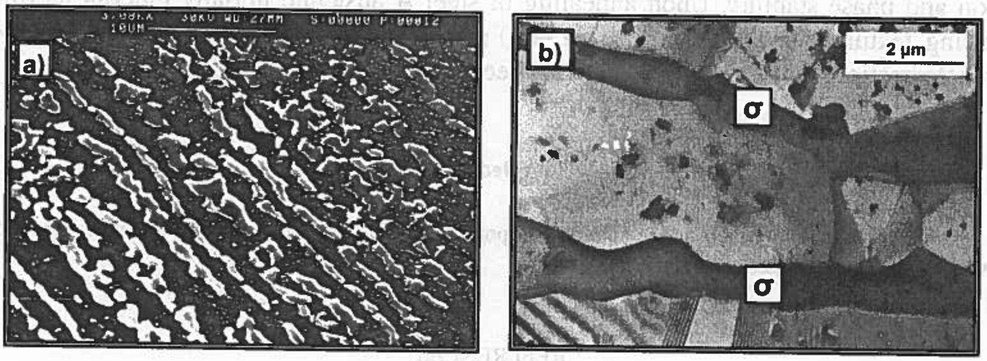

Fig. 5. Microstructures of steel B after 90% reduction and annealing at 700°C/10h; scanning and transmission electron microscopes, (a) and (b) respectively

The texture of austenite upon annealing of steel B seems unaffected by the precipitation processes (Fig. 2b). Texture changes after annealing at 700 and 850°C result mainly from recrystallization processes which proceed within the austenite bands formed upon cold-rolling. The austenite annealing texture describe the non-homogeneous α_1-fibre, with the strongest components from the range {110}<001>÷<115>, and the orientation components close to the {113}<332> from the limited {113}<uvw>-fibre, which are typical recrystallization components.

4. Concluding remarks

The appropriate temperature ranges for recrystallization annealing of ferrite-austenite duplex type steels depend on chemical and phase composition and should correspond to the temperatures at which precipitation of sigma phase is not observed.

Precipitation processes considerably change the phase composition and consequently affect the character of the structure and the annealing textures in 00H18N6Mo3 and 00H24N6 steels. Precipitation of σ-phase causes considerable weakening or even decay of ferrite diffraction peaks and influences mainly the ferrite annealing textures since it is formed at the expense of ferrite. The austenite annealing textures seem unaffected by σ-phase precipitation.

Recrystallization annealing of duplex type steels does not essentially change the band-like morphology of two-phase structure. Recrystallization processes of ferrite and austenite are limited to the bands of both phases formed in the course of cold-working. Significant changes of the austenite texture result mainly from recrystallization and are visible after prolonged annealing times or at higher temperatures since the formation of recrystallization nuclei is difficult in low stacking fault energy γ-phase.

Contribution of the inverse ($\alpha \rightarrow \gamma$) phase transformation into the texture formation results from the amount of strain induced α-phase and depends on chemical composition and phase stability. Upon annealing of steel A austenite initially inherits its own rolling texture due to the inverse ($\alpha \rightarrow \gamma$) transformation. The effect of the ($\alpha \leftrightarrow \gamma$) transformations on texture formation in steel B seems insignificant. .

Acknowledgements

The authors kindly acknowledge financial support from the Polish Committee of Scientific Research (KBN) under the contract No 11.110.230.

REFERENCES

[1] N. Akdut, J. Foct; ISIJ International **36**, 883-892 (1996).
[2] J. Keichel, J. Foct, G. Gottstein; ISIJ International **43**, 1781-1787 and 1788-1794 (2003).
[3] K. Tomimura, S. Takaki, Y. Tokunaga; ISIJ International **31**, 1431-1440 (1991).
[4] W. Reick, M. Pohl, A.F. Padilha, ISIJ International **38**, 567-571 (1998).
[5] T.H. Chen, J.R. Yang, Mater. Science and Eng. **311A**, 28-41 (2001).
[6] J. Ryś, M. Witkowska, W. Ratuszek, K. Chruściel, Mater. Konf. Spraw. PAN t.2, 294-300 (2002).
[7] M. Witkowska, J. Ryś, W. Ratuszek, K. Chruściel, Inż. Mater. **22**, 4, 950-953 (2001).
[8] W. Ratuszek, J. Ryś, M. Karnat, Archives of Metall. **45**, 57-70 (2000).

Received: 21 March 2005.